

Single Crystal Structure Investigations Under High-Pressure of the Mineral Cordierite with an Improved High-Pressure Cell

J. Koepke^{1*} and H. Schulz²

¹ Max-Planck-Institut für Festkörperforschung, 7000 Stuttgart 80, West Germany

² Institut für Kristallographie und Mineralogie, Universität München, 8000 München 2, West Germany

Abstract. An improved single-crystal high-pressure anvil cell with beryllium-gaskets was used for the investigations of structure and lattice parameters of cordierite which had been heated in an Ar stream at about 1,000° C to remove natural water from its structural channels. The influences of pressure transmitting media were studied by using water as a pressure medium at pressures of 0.3, 0.9, 1.2, and 2.3 GPa and fluorocarbon, a liquid consisting of large molecules, at 2.2 GPa. Water, but not fluorocarbon, is able to enter the channels in the cordierite structure. Large variations in the lattice constants resulted from changing the pressure medium used. A previously supposed discontinuity of the *b* lattice constant at nearly 0.3 GPa could not be established by the measurements taken so that there is no evidence for a phase transition at this pressure. Possibly the observed tilting of two tetrahedra against each other in this structure could have led to this misinterpretation. When water, but not fluorocarbon, is used as a pressure medium at 2.3 GPa, an additional electron density peak, presumably a water oxygen atom, appears in the channels. The water prevents the channels from shrinking and fixes their width at a value comparable to that of a naturally hydrated cordierite. In one of the silicate-tetrahedra the *Si-O* bond lengths are compressed almost 1 percent (2.3 GPa). This process may initiate a phase transition at higher pressures.

Introduction

Structural studies on cordierite have been carried out with neutron- and x-rays at normal conditions to study its channel constituents and Si/Al order/disorder (Cohen et al. 1977), and at high temperatures, to determine the origin of cordierite's unusually low rate of thermal expansion (Hochella et al. 1979). Furthermore, cordierites with different Fe/Mg compositions were investigated (Wallace and Wenk 1980). Work at high pressure has only been carried out by Mirwald et al. (1984), who determined the lattice constants of a cordierite from Soto/Argentina at different pressures. The results seemed to indicate the existence of two phase transitions as previously postulated by Mirwald (1982). Mirwald et al. stated that cordierite, forms two high pressure phases; one stable between 0.2 and 0.9 GPa and the other stable above 0.9 GPa. Both transitions were de-

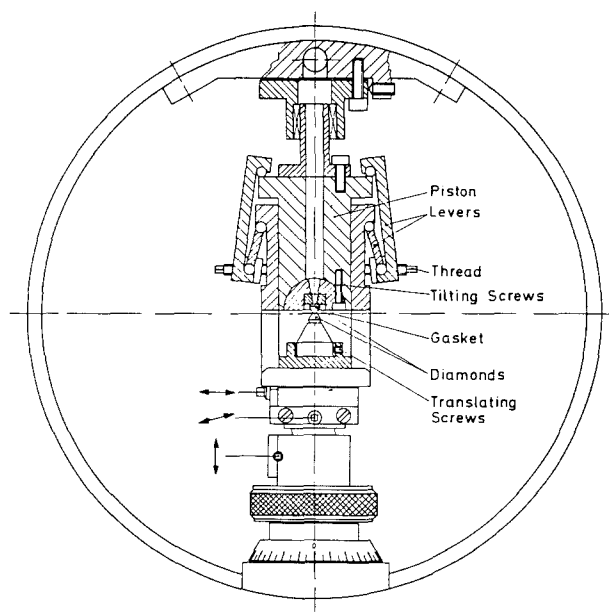


Fig. 1. Improved high-pressure diamond-anvil cell mounted on a Philips PW-1100 diffractometer (χ -circle with a diameter of 150 mm)

ected only as discontinuities of the compressibility, which suggests that they are second order. Structural studies at high pressure have never been undertaken for cordierite. The aim of the present study is to fill this omission with emphasis on the investigation of the purported phase transitions.

Only a small part of reciprocal space is accessible when using most high-pressure diamond anvil cells (Merrill and Basset 1974, Keller and Holzappel 1977). Therefore, most structural studies on minerals have been limited to crystals with high symmetry and small unit cells (Hazen and Finger 1982). Several attempts have been made to improve these limitations (Schiferl et al. 1978, Ahsbans 1984). All these new high-pressure cells as well as the cell used here (Dieterich et al. 1984, Koepke et al. 1985) have a new x-ray path in common. With our improved cell we are able to measure up to 95% of all non-Friedel reflections in a sufficient 2θ -range. This device, when mounted on a four-circle diffractometer (Fig. 1), enables us to investigate structures as complicated as orthorhombic cordierite. To overcome the effect

* Present address: Department of Chemistry, University of Pennsylvania, Philadelphia, PA 19104, USA

Table 1. Lattice constants and relative lattice constants for White Well and Zabargad cordierites

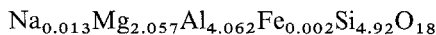
	0.1 MPa	0.3 GPa	0.9 GPa	1.2 GPa	2.3 GPa	2.2 GPa	
a (Å) ^a	17.079 (3)	17.071 (2)	17.058 (6)	17.040 (3)	17.013 (2)	16.990 (4)	16.975 (7) ^b
b (Å)	9.730 (2)	9.715 (1)	9.724 (3)	9.702 (2)	9.680 (1)	9.680 (2)	9.647 (4)
c (Å)	9.356 (2)	9.344 (1)	9.336 (3)	9.320 (2)	9.3035 (7)	9.293 (2)	9.274 (3)
V (Å ³)	1,554.8 (5)	1,549.7 (3)	1,548.6 (9)	1,540.8 (5)	1,532.2 (3)	1,528.4 (6)	1,518.7 (10)
a/a ₀	—	1	0.9992 (4)	0.9982 (2)	0.9966 (2)	0.9953 (3)	0.9944 (4)
b/b ₀	—	1	1.0009 (3)	0.9987 (2)	0.9964 (1)	0.9964 (2)	0.9930 (4)
c/c ₀	—	1	0.9991 (3)	0.9974 (2)	0.9957 (1)	0.9945 (2)	0.9925 (3)
V/V ₀	—	1	0.9993 (6)	0.9943 (4)	0.9887 (3)	0.9863 (4)	0.9800 (7)

^a Cohen et al.^b Measurements with fluorcarbon

of x-ray absorption by the gasket, especially at low Bragg angles, we used beryllium gaskets. This limited our maximum pressure to about 3 GPa.

Experimental

We used crystals from the island Zabargad/Red Sea (Kurat et al. 1982) that were kindly supplied by P.W. Mirwald, who heated the crystals in an Ar stream at about 1,000°C to remove the water from the channels in the structure. The chemical formula of this cordierite, the average from 17 microprobe analyses, is:



Thus we used a nearly pure Mg-cordierite, which is known to have an orthorhombic space group (*Cccm*).

The crystals had the shape of flat cylinders (about 100 µm in diameter and 60 µm in height), which allowed the application of a simple gasket-absorption algorithm. No absorption correction due to the crystal shape itself was made: with an absorption coefficient of only 8.724 cm⁻¹ for the Zabargad cordierite, intensity differences resulting from the different paths of the beams inside the crystal do not exceed about 3%.

The pressure was measured by the fluorescence of a small ruby splinter lying beside the sample in the gasket hole (Piermarini et al. 1975). An interferometer described by Keller and Holzapfel (1977) was used for measuring the shift of the ruby-fluorescence line. This system allowed pressure measurements with a standard deviation of ±0.07 GPa. This apparatus also had a systematic error of about ±2%. We therefore assumed an overall error of ±0.1 GPa.

Two different pressure transmitting media were used: (1) *water*, of which the molecules fit into the channels of the cordierite structure, and (2) *fluorcarbon*, a completely fluorinated cyclic ether, with molecules so large that they cannot enter the channels. The low solubility of water in fluorcarbon (13 ppm) ensures that the water contamination of fluorcarbon is negligible. Both media behave as liquids within the investigated pressure range (Piermarini et al. 1973 and own measurements). We applied pressures of 0.3, 0.9, 1.2, and 2.3 GPa with water as the pressure transmitting medium and of only 2.2 GPa with fluorcarbon.

Atomic positions of the cordierite structure are denoted with the nomenclature suggested by Cohen et al. (1977) and by Meagher and Gibbs (1977), with the exception that instead of *T* and *M*, the cations are labeled according to the atoms really found in a low-cordierite at these positions.

With respect to the values measured at pressures on the Zabargad cordierite, linear or quadratic regression lines, respectively, were calculated. In order to obtain comparable fluorcarbon curves we used all the values measured with water, except for the ones measured at the highest pressure reached (2.3 GPa), together with the only measurement at fluorcarbon pressure (2.2 GPa) in similar calculations. This must be allowed because, as is shown below, water is only found in the structure at 2.3 GPa. The curves in Figures 2–4, 6, and 8–10 calculated from measurements with water as a pressure transmitting medium are labeled by solid lines whereas fluorcarbon curves are indicated by dashed lines.

Lattice Parameters

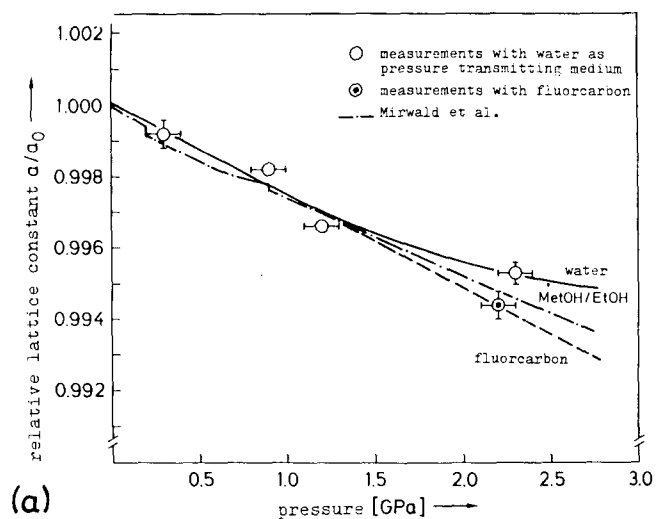
The lattice parameters, under ambient conditions and at the five different pressures, at which the structural investigations were carried out, were refined from the diffraction angles of about 50 reflections. The results are listed in Table 1. For comparison, the data of Cohen et al. (1977) for a White-Well cordierite/Australia are also shown.

The relative lattice constants and the unit cell volume are plotted against pressure in Figures 2 and 3, respectively. The bulk compressibility was computed between the two measurements at 0.3 and 0.9 and between 1.2 and the highest pressures reached: 2.3 GPa with water, and 2.2 GPa with fluorcarbon (Figure 4). According to Mirwald (1982), no phase transitions are to be expected in these two pressure-ranges.

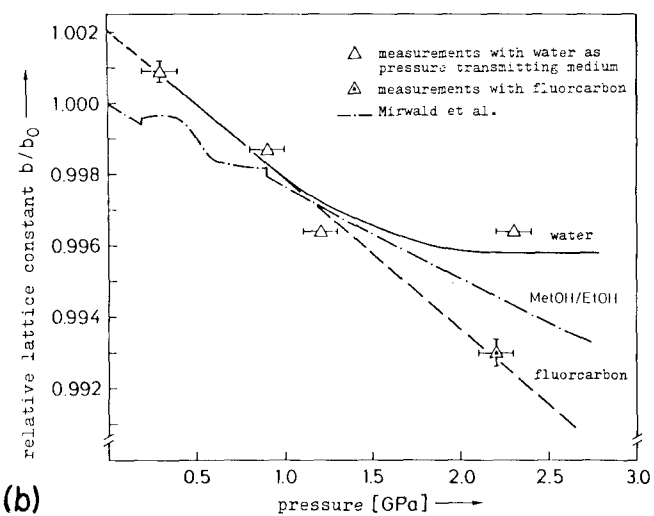
Structure Investigations

Diffraction intensities were collected on a Philips PW-1100 diffractometer for half the Ewald sphere with MoK_α-radiation up to sin θ/λ=0.8 for ambient conditions, sin θ/λ=0.6 for 0.3 GPa and sin θ/λ=0.7 for higher pressures. Data collection under high pressure was carried out using a special high-pressure control program executed on an external computer, that communicates with the Philips control computer via a serial interface (Koepeke 1985). The scans with 60 steps for each reflection were analyzed with the Lehmann-Larsen algorithm (Lehmann and Larsen 1974) integrated into the Prometheus program-system (Zucker et al. 1983). Symmetrical equivalent reflections were averaged by another part of the Prometheus system. For structure refinements we used the X-ray 72 program system (Stewart et al. 1972), with weights calculated according to

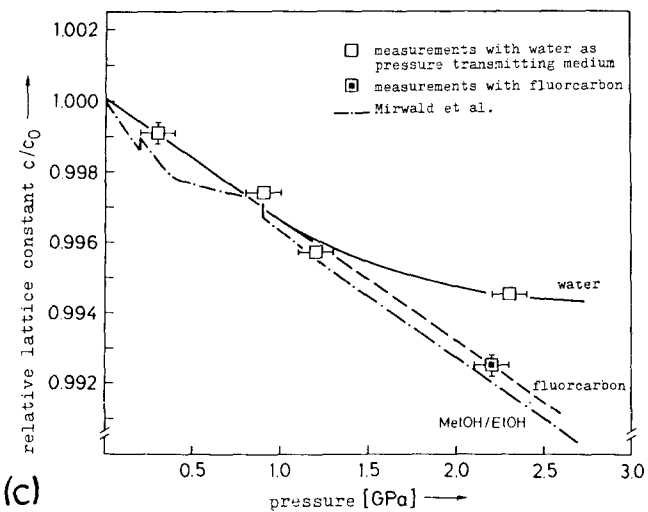
$$w = 1/\sqrt{\sigma^2(I_o) + (nI_o/100)^2}$$



(a)



(b)



(c)

Fig. 2a-c. Relative (a) a -, (b) b -, and (c) c -lattice constants vs. pressure

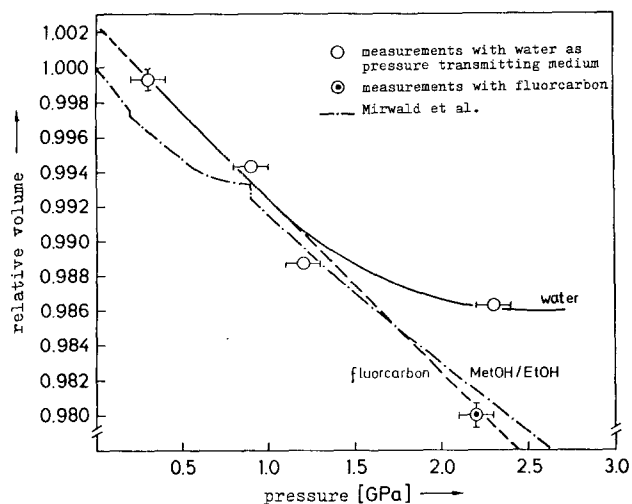


Fig. 3. Relative volume of the unit cell vs. pressure

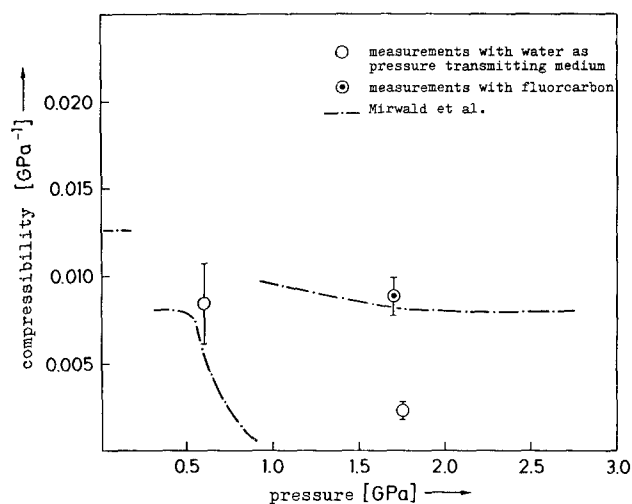


Fig. 4. Bulk compressibility vs. pressure

Table 2. Results of refinements for White-Well and Zabargad cordierites

Cordierite	Pressure	Pressure medium	Refined reflections	R	R_w
White-Well (Cohen et al.)	0.1 MPa	air	1,057	3.3	5.1
Zabargad	0.1 MPa	air	1,080	5.8	1.5
	0.3 GPa	water	492	10.2	11.6
	0.9 GPa	water	941	9.2	5.6
	1.2 GPa	water	934	7.9	2.2
	2.3 GPa	water	829	9.7	6.9
	2.2 GPa	fluorocarbon	495	11.0	7.7

A factor n between 0.5 and 1.5 helped to avoid overweighting of intense reflections. The refinement at 0.3 GPa was weighted with unit weights. Only reflections with intensities larger than 2 or 3 $\sigma(I_o)$, respectively, were allowed for the refinements, except for the data collected at 2.2 GPa with fluorocarbon, where reflections with $I_o \geq 5\sigma(I_o)$ were allowed.

Table 3. Final fractional coordinates and isotropic thermal parameters U ($\times 100$) for White Well and Zabargad cordierites at various pressures

Atom		0.1 MPa	0.3 GPa	0.9 GPa	1.2 GPa	2.3 GPa	2.2 GPa	
Al 11	x	0.25 ^a	0.25	0.25	0.25	0.25	0.25 ^b	
	y	0.25	0.25	0.25	0.25	0.25	0.25	
	z	0.2501 (1)	0.2505 (3)	0.2493 (11)	0.2500 (3)	0.2503 (3)	0.2503 (5)	0.2473 (10)
	U ^c	0.66	0.75 (4)	1.38 (20)	0.74 (6)	0.72 (5)	0.75 (10)	0.76 (16)
Si 16	x	0.0	0.0	0.0	0.0	0.0	0.0	
	y	0.5	0.5	0.5	0.5	0.5	0.5	
	z	0.25	0.25	0.25	0.25	0.25	0.25	
	U	0.57	0.67 (5)	1.33 (26)	0.63 (8)	0.61 (7)	0.81 (13)	0.32 (20)
Si 21	x	0.1926 (1)	0.19281 (9)	0.1938 (5)	0.1930 (1)	0.1930 (1)	0.1932 (2)	0.1938 (4)
	y	0.0778 (1)	0.0782 (2)	0.0778 (8)	0.0780 (3)	0.0779 (2)	0.0769 (4)	0.0770 (8)
	z	0.0	0.0	0.0	0.0	0.0	0.0	0.0
	U	0.49	0.53 (4)	1.33 (21)	0.55 (6)	0.42 (5)	0.60 (10)	0.63 (17)
Al 26	x	0.0508 (1)	0.0506 (1)	0.0501 (5)	0.0509 (2)	0.0506 (1)	0.0514 (2)	0.0520 (5)
	y	0.3079 (1)	0.3085 (2)	0.3073 (9)	0.3077 (3)	0.3083 (3)	0.3076 (5)	0.3055 (9)
	z	0.0	0.0	0.0	0.0	0.0	0.0	0.0
	U	0.55	0.62 (4)	0.96 (21)	0.58 (6)	0.51 (6)	0.63 (11)	0.69 (19)
Si 23	x	-0.1352 (1)	-0.13544 (9)	-0.1354 (5)	-0.1352 (1)	-0.1351 (1)	-0.1350 (2)	-0.1348 (4)
	y	0.2375 (1)	0.2376 (2)	0.2376 (8)	0.2378 (3)	0.2374 (2)	0.2368 (4)	0.2369 (8)
	z	0.0	0.0	0.0	0.0	0.0	0.0	0.0
	U	0.49	0.60 (4)	1.17 (20)	0.64 (6)	0.57 (5)	0.62 (10)	0.11 (15)
O 11	x	0.2474 (1)	0.2468 (1)	0.2483 (8)	0.2473 (2)	0.2474 (2)	0.2476 (3)	0.2473 (7)
	y	0.1029 (1)	0.1029 (2)	0.1038 (12)	0.1032 (4)	0.1031 (3)	0.1022 (6)	0.1033 (10)
	z	0.1410 (2)	0.1407 (3)	0.1416 (15)	0.1416 (4)	0.1421 (3)	0.1420 (6)	0.1426 (12)
	U	0.87	0.83 (6)	1.25 (31)	0.71 (10)	0.68 (8)	0.92 (16)	0.58 (26)
O 16	x	0.0620 (1)	0.0625 (1)	0.0611 (8)	0.0618 (2)	0.0624 (2)	0.0625 (3)	0.0625 (7)
	y	0.4160 (2)	0.4156 (2)	0.4167 (13)	0.4158 (4)	0.4154 (3)	0.4157 (6)	0.4152 (11)
	z	0.1512 (2)	0.1506 (3)	0.1509 (17)	0.1511 (5)	0.1506 (4)	0.1503 (7)	0.1502 (12)
	U	0.87	0.84 (6)	1.72 (35)	0.84 (10)	0.78 (9)	0.75 (17)	0.65 (27)
O 13	x	-0.1732 (1)	-0.1733 (1)	-0.1737 (10)	-0.1733 (2)	-0.1733 (2)	-0.1734 (3)	-0.1734 (6)
	y	0.3101 (2)	0.3100 (2)	0.3088 (14)	0.3110 (4)	0.3116 (3)	0.3138 (7)	0.3127 (10)
	z	0.1416 (2)	0.1413 (3)	0.1424 (16)	0.1410 (5)	0.1423 (3)	0.1415 (7)	0.1414 (13)
	U	0.89	0.77 (6)	2.09 (37)	0.67 (10)	0.78 (9)	1.22 (18)	0.55 (27)
O 21	x	0.1223 (1)	0.1226 (2)	0.1223 (15)	0.1228 (3)	0.1228 (2)	0.1239 (5)	0.1227 (9)
	y	0.1839 (2)	0.1846 (3)	0.1880 (21)	0.1842 (7)	0.1851 (5)	0.1825 (10)	0.1833 (16)
	z	0.0	0.0	0.0	0.0	0.0	0.0	0.0
	U	1.32	1.12 (10)	2.17 (52)	1.00 (14)	1.12 (13)	0.99 (24)	0.50 (37)
O 26	x	-0.0430 (1)	-0.0433 (2)	-0.0440 (11)	-0.0431 (3)	-0.0428 (3)	-0.0424 (5)	-0.0430 (10)
	y	0.2476 (2)	0.2491 (3)	0.2515 (21)	0.2485 (7)	0.2480 (5)	0.2462 (11)	0.2441 (19)
	z	0.0	0.0	0.0	0.0	0.0	0.0	0.0
	U	1.23	1.17 (10)	0.92 (42)	1.16 (15)	0.82 (12)	1.29 (25)	1.82 (45)
O 23	x	-0.1645 (1)	-0.1638 (2)	-0.1646 (13)	-0.1650 (4)	-0.1647 (3)	-0.1656 (5)	-0.1646 (11)
	y	0.0792 (2)	0.0803 (4)	0.0793 (20)	0.0795 (7)	0.0806 (5)	0.0778 (10)	0.0812 (19)
	z	0.0	0.0	0.0	0.0	0.0	0.0	0.0
	U	1.22	1.35 (10)	1.53 (47)	0.99 (15)	1.06 (13)	1.32 (26)	0.98 (41)
Mg	x	0.1625 (1)	0.16248 (9)	0.1629 (6)	0.1626 (2)	0.1622 (1)	0.1624 (2)	0.1622 (5)
	y	0.5	0.5	0.5	0.5	0.5	0.5	0.5
	z	0.25	0.25	0.25	0.25	0.25	0.25	0.25
	U	0.74	0.88 (4)	1.46 (23)	0.69 (7)	0.69 (6)	0.84 (11)	0.74 (18)

^a Cohen et al.^b measurements with fluorocarbon^c multiplied with factor 100

The refinements were conducted by minimizing the value of $\sum_{hkl} w(|F_o| - |F_c|)^2$

Final R_w or R values are listed in Table 2. Values of Cohen et al. (1977) are also listed for comparison. The experimental procedures were detailed by Koepke (1985).

The final positional parameters and isotropic temperature factors are listed together with the corresponding values from Cohen et al. (1977) in Table 3. Bond lengths and bond angles are given in Tables 4 and 5. Selected inter-tetrahedral or octahedral angles that show the tiltings of the adjacent polyhedra are listed in Table 6.

Table 4. Bondlengths (Å) for White-Well and Zabargad cordierites at various pressures

Bonding	Mult.	0.1 MPa		0.3 GPa	0.9 GPa	1.2 GPa	2.3 GPa	2.2 GPa
Al 11—O 11	2	1.760 (2) ^a	1.760 (3)	1.741 (14)	1.747 (4)	1.742 (3)	1.750 (6)	1.717 (12) ^b
—O 13	2	1.757 (2)	1.755 (3)	1.745 (17)	1.759 (4)	1.749 (3)	1.757 (6)	1.768 (12)
mean		1.759 (1)	1.758 (2)	1.743 (9)	1.753 (2)	1.746 (2)	1.754 (4)	1.743 (7)
Si 16—O 16	4	1.626 (2)	1.635 (2)	1.612 (14)	1.621 (4)	1.628 (3)	1.629 (6)	1.629 (6)
Si 21—O 11	2	1.636 (2)	1.623 (3)	1.637 (15)	1.630 (4)	1.632 (3)	1.629 (6)	1.624 (12)
—O 23'	1	1.601 (2)	1.617 (4)	1.606 (22)	1.601 (7)	1.607 (6)	1.569 (11)	1.604 (19)
—O 21	1	1.583 (2)	1.583 (3)	1.623 (25)	1.580 (7)	1.583 (5)	1.558 (10)	1.584 (17)
mean		1.614 (1)	1.612 (2)	1.626 (11)	1.610 (3)	1.614 (3)	1.596 (5)	1.609 (9)
Al 26—O 16	2	1.773 (2)	1.762 (3)	1.776 (16)	1.766 (5)	1.755 (4)	1.755 (7)	1.759 (12)
—O 21	1	1.716 (2)	1.720 (4)	1.691 (25)	1.713 (7)	1.712 (5)	1.729 (10)	1.682 (18)
—O 26	1	1.706 (2)	1.704 (4)	1.694 (21)	1.701 (7)	1.693 (5)	1.701 (9)	1.718 (20)
mean		1.742 (1)	1.737 (2)	1.734 (12)	1.737 (4)	1.729 (3)	1.735 (5)	1.730 (9)
Si 23—O 13	2	1.634 (2)	1.629 (3)	1.635 (16)	1.629 (5)	1.640 (3)	1.646 (7)	1.638 (12)
—O 23	1	1.619 (2)	1.603 (4)	1.618 (22)	1.617 (7)	1.600 (6)	1.625 (11)	1.585 (19)
—O 26	1	1.578 (2)	1.577 (4)	1.567 (20)	1.573 (6)	1.574 (5)	1.576 (9)	1.561 (19)
mean		1.616 (1)	1.610 (2)	1.614 (11)	1.612 (3)	1.614 (3)	1.623 (5)	1.606 (9)
Mg —O 16	2	2.113 (2)	2.109 (3)	2.128 (16)	2.114 (5)	2.101 (4)	2.098 (6)	2.094 (13)
—O 11	2	2.100 (2)	2.108 (3)	2.082 (15)	2.093 (5)	2.090 (3)	2.080 (6)	2.085 (13)
—O 13'	2	2.115 (2)	2.115 (2)	2.121 (14)	2.104 (4)	2.090 (3)	2.074 (7)	2.077 (10)
mean		2.109 (1)	2.111 (1)	2.110 (7)	2.104 (2)	2.093 (2)	2.085 (3)	2.085 (5)

^a Cohen et al.^b measurements with fluorcarbon**Table 5.** Bondangles (°) for White Well and Zabargad cordierites at various pressures

Cation	Anions	Mult.	0.1 MPa		0.3 GPa	0.9 GPa	1.2 GPa	2.3 GPa	2.2 GPa
Al 11	O 13''—O 13'''	1	109.6 (1) ^a	109.6 (2)	109.2 (9)	109.4 (2)	110.3 (2)	110.2 (4)	108.5 (7) ^b
	O 11 —O 13''	2	94.7 (1)	95.1 (1)	94.5 (6)	94.5 (2)	94.1 (1)	93.4 (3)	93.9 (5)
	O 11 —O 13''	2	125.9 (1)	125.6 (1)	126.2 (7)	126.1 (2)	126.1 (1)	126.8 (3)	126.3 (5)
	O 11 —O 11'	1	109.0 (1)	108.7 (2)	109.5 (8)	109.5 (8)	109.3 (2)	109.4 (2)	109.8 (4)
Si 16	O 16 —O 16'	2	110.7 (1)	110.8 (1)	110.0 (8)	110.7 (2)	110.8 (2)	110.6 (3)	110.7 (6)
	O 16 —O 16''	2	119.7 (1)	119.8 (1)	119.6 (7)	119.4 (2)	119.6 (2)	119.9 (3)	119.7 (5)
	O 16 —O 16'''	2	98.7 (1)	98.5 (1)	99.5 (7)	98.9 (2)	98.7 (2)	98.6 (3)	98.6 (6)
Si 21	O 11 —O 21	2	109.7 (1)	109.4 (1)	109.0 (7)	109.4 (2)	109.3 (2)	109.2 (3)	108.9 (6)
	O 11 —O 23	2	108.3 (1)	108.4 (1)	108.8 (7)	108.2 (2)	108.2 (2)	108.2 (3)	108.8 (6)
	O 11 —O 11 ^m	1	107.4 (1)	108.2 (1)	107.7 (9)	108.1 (2)	108.2 (2)	108.2 (3)	109.1 (7)
	O 21 —O 23	1	113.3 (1)	112.9 (2)	113.3 (12)	113.4 (4)	113.5 (3)	113.6 (5)	112.4 (10)
Al 26	O 16 —O 21	2	109.9 (1)	109.4 (1)	109.5 (7)	109.9 (2)	109.3 (2)	109.9 (3)	110.4 (6)
	O 16 —O 26	2	107.8 (1)	107.9 (1)	106.9 (7)	107.5 (2)	108.2 (2)	108.0 (3)	107.6 (6)
	O 16 —O 16 ^m	1	105.8 (1)	106.0 (1)	105.1 (8)	105.8 (3)	106.0 (2)	105.4 (4)	104.7 (7)
	O 21 —O 26	1	115.2 (1)	115.8 (2)	118.0 (11)	115.9 (4)	115.7 (3)	115.0 (5)	115.4 (9)
Si 23	O 13 —O 26	2	111.6 (1)	111.4 (1)	111.2 (7)	111.6 (2)	111.5 (2)	111.7 (3)	112.3 (6)
	O 13 —O 23	2	106.8 (1)	107.0 (1)	106.3 (7)	106.8 (2)	106.9 (2)	107.6 (3)	107.2 (6)
	O 13 —O 13 ^m	1	108.2 (1)	108.2 (1)	108.8 (9)	107.6 (3)	107.7 (2)	106.1 (4)	106.4 (7)
	O 26 —O 23	1	111.5 (1)	111.6 (2)	112.9 (12)	112.1 (4)	112.1 (3)	111.9 (6)	111.1 (10)
Mg	O 11 —O 13'	2	96.9 (1)	96.7 (1)	97.6 (6)	96.9 (2)	96.9 (1)	96.5 (2)	96.7 (5)
	O 16 —O 11	2	101.4 (1)	101.4 (1)	101.4 (5)	101.6 (2)	101.4 (1)	101.4 (2)	101.4 (4)
	O 13' —O 16	2	101.4 (1)	101.4 (1)	101.5 (6)	101.3 (2)	101.6 (1)	101.3 (2)	101.5 (5)
	O 11 —O 11'	1	85.8 (1)	85.4 (1)	86.7 (6)	85.7 (2)	85.3 (1)	85.3 (3)	85.0 (5)
	O 16 —O 13'''	2	86.7 (1)	86.7 (1)	86.7 (6)	86.8 (2)	86.8 (1)	87.1 (2)	87.0 (4)

^a Cohen et al.^b measurements with fluorcarbon

Table 6. Selected inter-tetrahedral or octahedral angles respectively for White Well and Zabargad cordierites

Anion	Cations	Mult.	0.1 MPa	0.3 GPa	0.9 GPa	1.2 GPa	2.3 GPa	2.2 GPa	
Six-membered ring									
O 21'	Si 21—Al 26'	2	176.0 (2) ^a	176.4 (2)	178.0 (16)	176.4 (5)	176.8 (4)	176.5 (7)	175.9 (12) ^b
O 23	Si 21—Si 23	2	179.5 (2)	179.7 (3)	179.9 (9)	181.0 (5)	180.9 (4)	182.2 (6)	180.6 (13)
O 26	Si 23—Al 26	2	163.5 (2)	164.3 (2)	166.3 (15)	164.1 (5)	163.6 (4)	162.9 (8)	162.4 (13)
Six-membered ring against octahedron									
O 11	Si 21—Mg	2	137.7 (1)	137.7 (1)	137.0 (8)	137.4 (3)	137.3 (2)	137.4 (4)	136.6 (7)
O 13'	Si 23—Mg	2	137.0 (1)	137.0 (1)	136.2 (9)	137.4 (3)	137.2 (2)	138.3 (4)	137.7 (7)
O 16	Al 26—Mg	2	131.8 (1)	132.4 (1)	131.2 (8)	131.5 (2)	132.4 (2)	132.1 (3)	131.9 (7)
Four-membered ring against octahedron									
O 11	Al 11—Mg	2	95.0 (1)	94.6 (1)	95.9 (7)	95.2 (2)	95.4 (1)	95.4 (3)	96.0 (5)
O 13	Al 11—Mg	2	94.5 (1)	94.5 (1)	94.5 (7)	94.5 (2)	95.2 (2)	95.4 (3)	94.7 (5)
O 16	Si 16—Mg	2	94.9 (1)	94.8 (1)	95.0 (7)	94.9 (2)	94.7 (2)	94.7 (3)	94.6 (5)
Four-membered against six-membered ring									
O 16	Si 16—Al 26	2	132.9 (1)	132.4 (1)	133.6 (9)	133.2 (3)	132.6 (2)	132.9 (3)	133.3 (7)
O 11	Al 11—Si 21	2	127.2 (1)	127.6 (1)	127.0 (9)	127.3 (3)	127.2 (2)	127.0 (4)	127.2 (7)
O 13	Al 11'—Si 23	2	128.2 (1)	128.3 (1)	129.1 (9)	128.0 (3)	127.4 (2)	126.3 (4)	127.5 (7)

^a Cohen et al.^b measurements with fluorcarbon

Discussion

The structure of cordierite is built up of (Si,Al)O₄ tetrahedra and MgO₆ octahedra. Figure 5 shows an ideal cordierite structure projected onto (001). Rings composed of six corner-linked tetrahedra are superimposed along the *c* axis to form the channels in the structure. The rings are included in a frame of edge-sharing octahedra and tetrahedra, with the octahedra located between the ring planes. Because of the higher compressibility of the octahedra compared to the tetrahedra (comp. Fig. 6a with b and c) this frame contracts more with pressure than the six-membered rings. Consequently, the six-membered rings are constrained by this frame so long as the symmetry of the structure is preserved. We were therefore able to simulate this pressure effect in the two-dimensional model shown in Figure 5 by giving the ring-tetrahedron projections a somewhat larger size, while keeping the frame size constant. Thus, the two-fold symmetry of the rings, perpendicular to the mirror-planes on which they lie, require that at least two tetrahedra of the ring shown in Figure 5 have to shrink in their projection onto (001). Our structure investigations verified this simple model.

When water is the pressure medium at 2.3 GPa, the weighted difference Fourier map shows a significant electron density (Fig. 7a) in the channel, whereas when fluorcarbon is the pressure medium, no such electron density (Fig. 7b) is observed at comparable pressures. The additional electron density can be refined as water oxygen (O_w) with a population of 0.10(2) and a mean square displacement of $U=0.03$ at $x=\pm 0.053(2)$, $y=0$, and $z=1/4$. This indicates that water molecules really penetrate into the structure.

The cross section of the six-membered ring approaches a constant value above 1.2 GPa water pressure as shown by the *O-O* distances directly across the channel (Fig. 8). The *O-O* distances reached are comparable to those of cordierite bearing a natural water (Cohen et al. 1977). Probab-

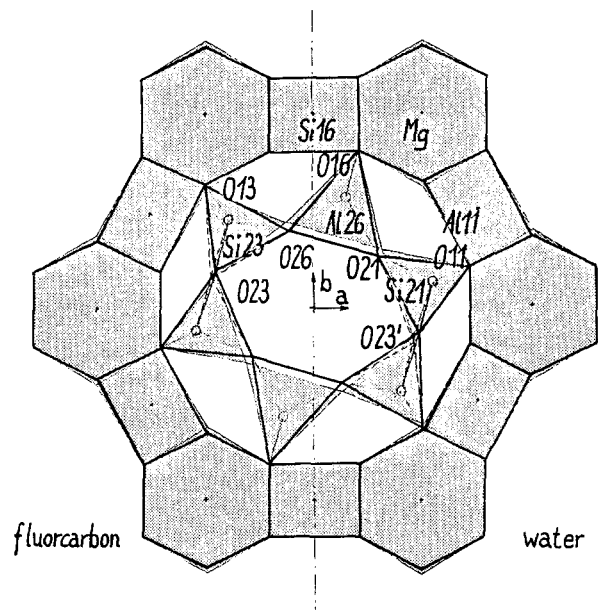


Fig. 5. Detail of an ideal cordierite structure projected onto (001). The triangles and squares are tetrahedra projected along their threefold or fourfold axes, respectively, on a plane perpendicular to this axis, while hexagons are octahedra projected along their threefold axes. Shaded areas symbolize ambient conditions. Solid lines indicate changes in the structural projection with the pressure transmitting medium (left side: fluorcarbon, right side: water)

ly hydrogen bonds are formed. Only O(23) seems to be too far away to be involved. With fluorcarbon as the pressure medium, however, the *O-O* distances decrease further (Fig. 8).

The different behavior of the structure due to the pressure medium is also reflected in the lattice parameters. The curves of all three lattice constants and the unit cell volume

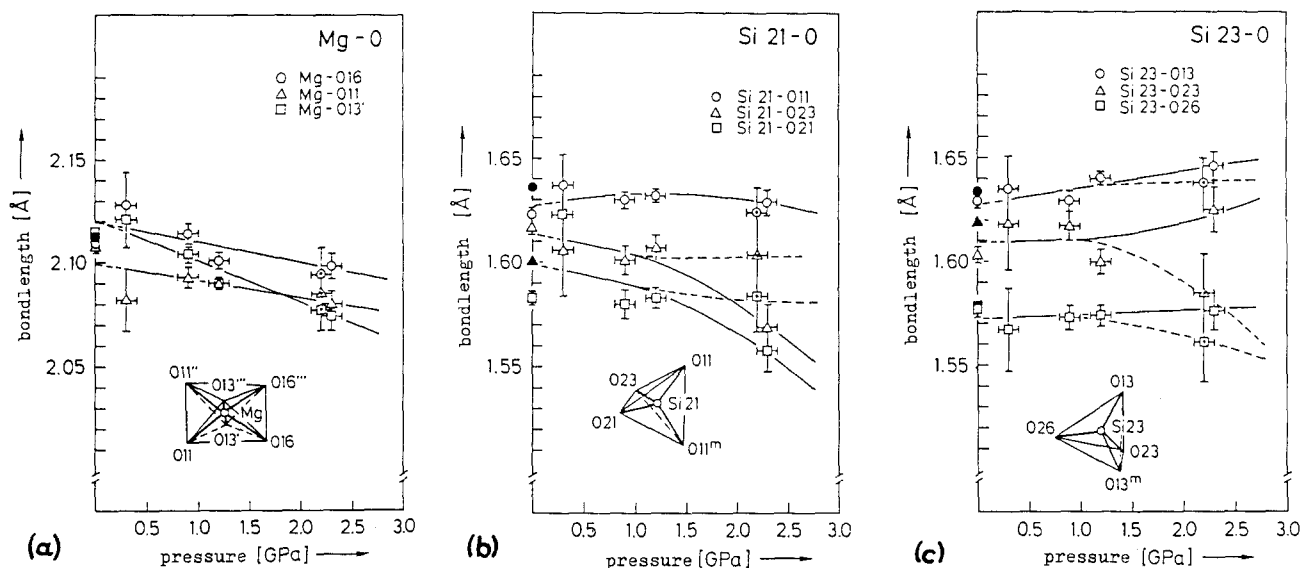


Fig. 6a-c. Bond lengths in the (a) Mg-octahedron, (b) Si(21) tetrahedron, and (c) Si(23) tetrahedron vs. pressure

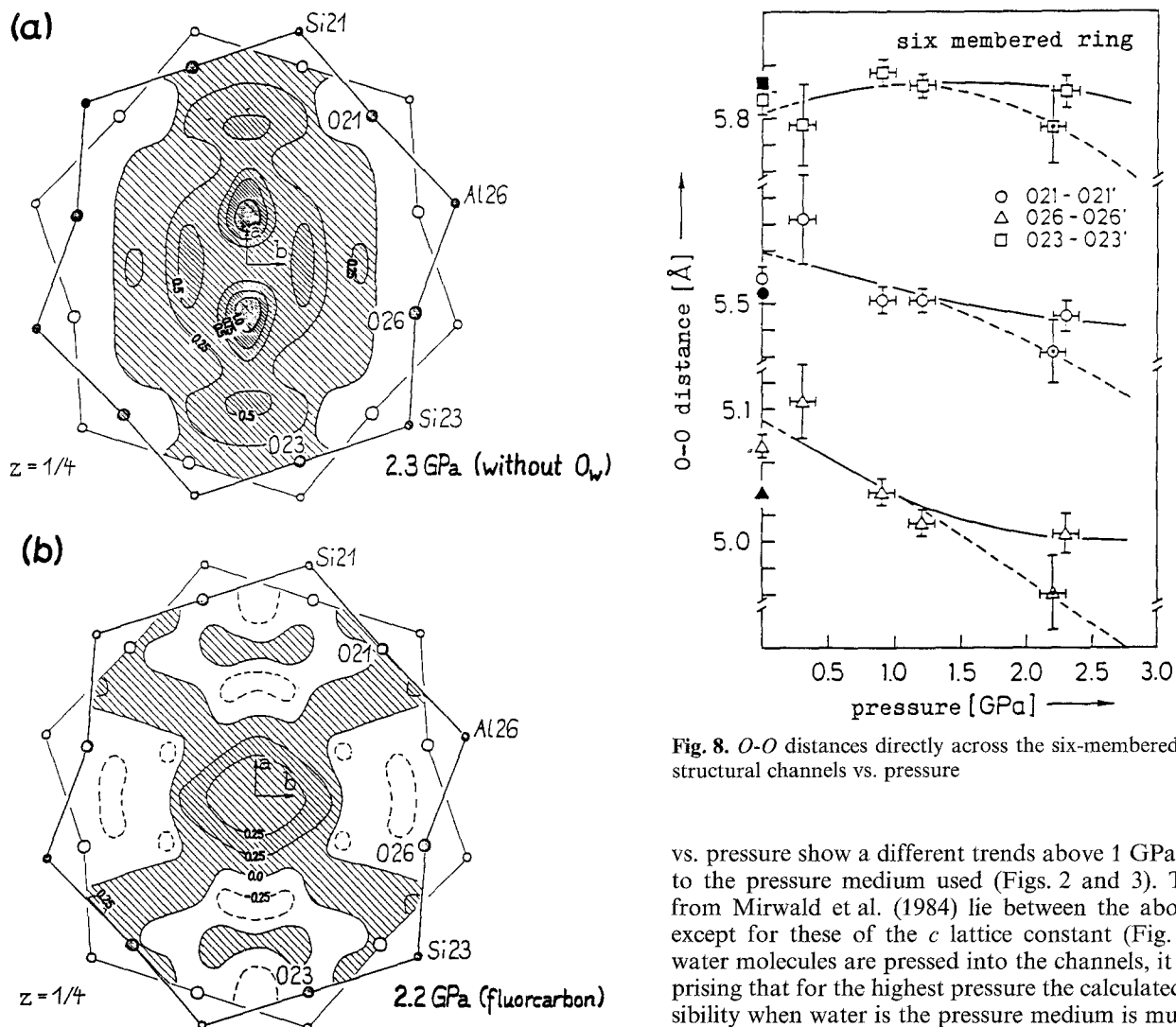


Fig. 8. O-O distances directly across the six-membered ring in the structural channels vs. pressure

Fig. 7a, b. Weighted difference fourier maps at (a) 2.3 GPa with water (without O_w) and at (b) 2.2 GPa with fluorocarbon as pressure medium. The difference between two adjacent lines is $0.25 e/\text{\AA}^3$. Areas with positive electron density are shaded

vs. pressure show a different trends above 1 GPa according to the pressure medium used (Figs. 2 and 3). The curves from Mirwald et al. (1984) lie between the above curves, except for these of the c lattice constant (Fig. 2c). Since water molecules are pressed into the channels, it is not surprising that for the highest pressure the calculated compressibility when water is the pressure medium is much smaller than that when fluorocarbon is the pressure medium (Fig. 4). Yet, unexpectedly, the water molecules are unable to enter the channels in significant amounts for pressures lower than about 1 GPa, as indicated by the coincidence of the fluor-

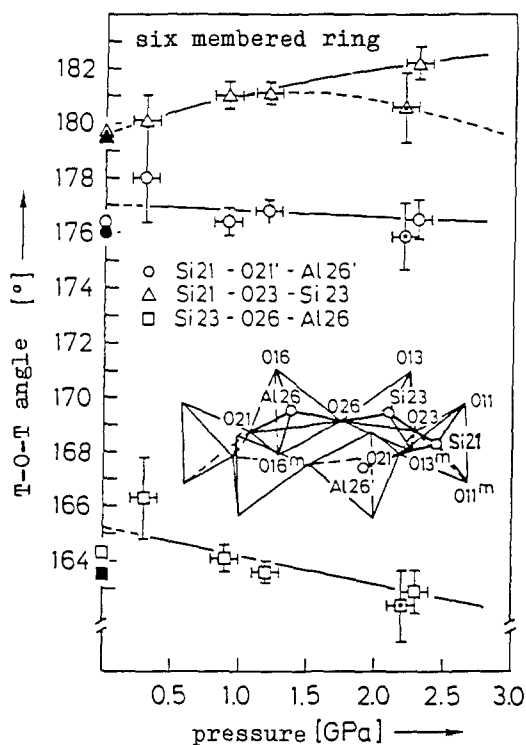


Fig. 9. $T-O-T$ angles vs. pressure indicating the tilting of the tetrahedra belonging to the six-membered ring against each other

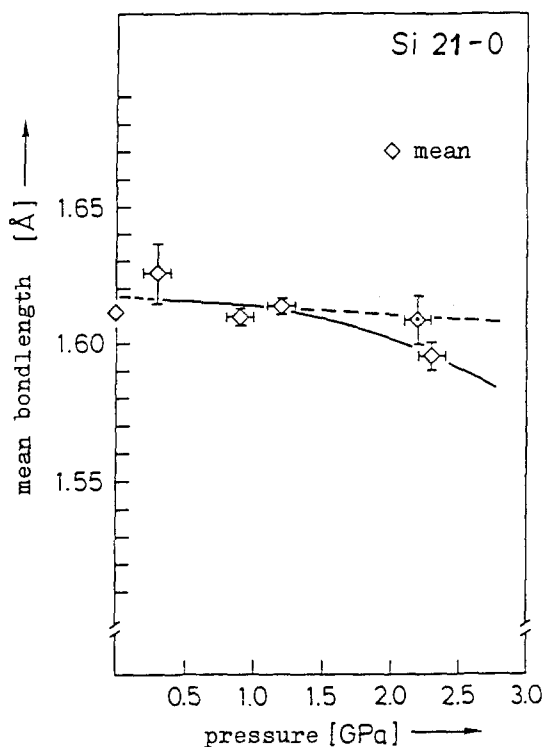


Fig. 10. Mean bond length of the Si(21) tetrahedron vs. pressure

carbon curves and the corresponding water curves up to this pressure (Figs. 2 and 3). Mirwald et al. (1984) used an alcohol-mixture (methanol/ethanol) as their pressure transmitting medium. The position of their curves just between the curves we found may be explained by assuming that methanol, but not ethanol, is small enough to penetrate the cordierite channels.

The cordierite structure reacts to pressure, as is expected from the simple model described above (Fig. 5). With water as a pressure medium, the projections of the Si(21) tetrahedron onto (001) are reduced in size, while the size of the Si(23) tetrahedron remains constant. The converse is true for fluorocarbon: the projections of the Si(21) tetrahedron remain nearly unchanged, while the Si(23) tetrahedron projections shrink.

The $Si-O$ bond lengths of the two tetrahedra in Figures 6b and c corroborate this statement. With water as the pressure medium, the bond lengths Si(21) - O(23) and Si(21) - O(21) (Fig. 6b), which lie in the plane of the above mentioned projection, decrease, while the corresponding bonds Si(23) - O(23) and Si(23) - O(26) (Fig. 6c) remain nearly constant or grow even larger. With fluorocarbon, on the other hand, the respective bond lengths related to the Si(23) tetrahedron decrease and those to the Si(21) tetrahedron remain constant.

According to our model (Fig. 5), the pressure transmitting medium also influences the tilting of the two tetrahedra, Si(21) and Si(23), against each other. When water is the pressure medium (right side Fig. 5), the tetrahedra have to tilt towards the frame; with fluorocarbon (left side Fig. 5) these tetrahedra tilt towards the middle of the six-membered ring.

This is reflected in the measurements of the angle Si(21) - O(23) - Si(23) (Fig. 9), which increases with the amount of water present in the channel, while it remains nearly constant with fluorocarbon as the pressure transmitting medium. In the latter case the curve decreases at even higher pressures. Remarkably, when water is the pressure medium this angle varies through the extreme value of 180° where the three atoms are linearly arranged. This value is reached at about 0.3 GPa.

Because the above line must be nearly parallel to the b axis, it is plausible that this structural change influences the b lattice constant. In fact, the b lattice constant (Fig. 2b) and the volume (Fig. 3) vary with water pressures in curves that do not extrapolate to unity at ambient conditions. A comparable observation for the b lattice constant apparently led Mirwald (1982) to the assumption that cordierite undergoes a first phase transition at 0.2 GPa. However, because the change of the angle Si(21) - O(23) - Si(23), which in our opinion is mainly responsible for this observation, seems to proceed continuously, and since we did not find any other significant structural change at 0.3 GPa, we cannot support the existence of the phase transition postulated by Mirwald.

A second phase transition postulated by Mirwald (1982) and assumed to occur at about 1 GPa was not observed either. With water as pressure medium, not only is the projection of the Si(21) tetrahedron onto (001) reduced, but its mean bond length (Fig. 10) indicates that the entire tetrahedron significantly shrinks with pressure (it is reduced by about 1 percent at 2.3 GPa). Perhaps a phase transition, comparable to the second phase transition postulated by Mirwald (1982), is introduced by this process. Unfortunately,

ly, the beryllium-gaskets we used, however, did not permit us to increase the pressure to values at which this hypothesis could be tested.

References

- Asbahi H (1984) Diamond-anvil high-pressure cell for improved single crystal x-ray diffraction measurements. *Rev Sci Instrum* 55:99–102
- Cohen JP, Ross FK, Gibbs GV (1977) An x-ray and neutron diffraction study of hydrous low cordierite. *Am Mineral* 62:67–75
- Dieterich W, Glinnemann J, Koepke J, Schulz H (1984) An improved diamond anvil high-pressure cell for single crystal work. *Acta Crystallogr A* 40(Suppl):C-413
- Hazen RM, Finger LW (1982) Comparative crystal chemistry. John Wiley and Sons, New York pp 149–151
- Hochella MF, Brown GE, Ross FK, Gibbs GV (1979) High-temperature crystal chemistry of hydrous Mg- and Fe-cordierites. *Am Mineral* 64:337–351
- Keller R, Holzappel WB (1977) Diamond anvil device for x-ray diffraction on single crystals under pressure up to 100 kilobar. *Rev Sci Instrum* 48:517–523
- Koepke J (1985) Einkristall-Strukturuntersuchungen unter hydrostatischem Druck am Mineral Cordierit mit einer verbesserten Hochdruckzelle. Dissertation Universität Hamburg
- Koepke J, Dieterich W, Glinnemann J, Schulz H (1985) Improved diamond-anvil high-pressure cell for single crystal work. *Rev Sci Instrum* 56:2119–2122
- Kurat G, Niedermayer G, Prinz M (1982) Peridot von Zabargad, Rotes Meer. *Aufschluss* 33:169–182
- Lehmann MS, Larsen FK (1974) A method for location of the peaks in step-scan-measured Bragg reflections. *Acta Crystallogr A* 30:580–584
- Meagher EP, Gibbs GV (1977) The polymorphism of cordierite: II. The crystal structure of indialite. *Can Mineral* 15:43–49
- Merill L, Bassett WA (1974) Miniature diamond anvil pressure cell for single crystal x-ray diffraction studies. *Rev Sci Instrum* 45:290–294
- Mirwald PW (1982) High-pressure phase transitions in cordierite. *Phys Earth Planet Int* 29:1–5
- Mirwald PW, Malinowski M, Schulz H (1984) Isothermal compression of low-cordierite to 30 kbar (25° C). *Phys Chem Minerals* 11:140–148
- Piermarini GJ, Block S, Barnett JD, Forman RA (1975) Calibration of the pressure dependence of the R₁ ruby fluorescence line to 195 kbar. *J Appl Phys* 46:2774–2780
- Schiferl D, Jamieson JC, Lenco JE (1978) 90-Kilobar diamond-anvil high-pressure cell for use on an automatic diffractometer. *Rev Sci Instrum* 49:359–364
- Stewart JM, Kruger GJ, Ammon HL, Dickson C, Hall SR (1972) The x-ray system. Computer Science Center, University of Maryland, Technical Report TR-192
- Wallace JH, Wenk HR (1980) Structure variation in low cordierites. *Am Mineral* 65:96–111
- Zucker UH, Perenthaler E, Kuhs WF, Bachmann R, Schulz H (1983) A program system for investigation of anharmonic thermal vibrations in crystals. *J Appl Crystallogr* 16:358

Received May 13, 1985